

# Single production of excited electrons at future $e^-e^+$ , $ep$ and $pp$ colliders

O. Çakır\* and A. Yilmaz

Ankara University, Faculty of Sciences, Department of Physics, 06100, Tandoğan, Ankara, Turkey

S. Sultansoy†

Gazi University, Faculty of Arts and Sciences, Department of Physics, 06500, Teknikokullar, Ankara, Turkey. and Azerbaijan Academy of Sciences, Institute of Physics, H. Cavid Ave. 33, Baku, Azerbaijan.

We analyzed the potential of the NLC with  $\sqrt{s} = 0.5$  TeV, NLC  $\times$  LHC based  $ep$  collider with  $\sqrt{s} = 3.74$  TeV and LHC with  $\sqrt{s} = 14$  TeV to search for excited electrons through transition magnetic type couplings with gauge bosons. The  $e^* \rightarrow e\gamma$  signal and corresponding backgrounds are studied in detail.

## I. INTRODUCTION

Three types of colliders related to the energy frontiers in particle physics research seem to be promising in the next decade. Namely, Large Hadron Collider (LHC) with the center of mass energy  $\sqrt{s} = 14$  TeV and luminosity  $L = 10^{34} - 10^{35} \text{ cm}^{-2} \text{ s}^{-1}$ , Next Linear Collider (NLC) with  $\sqrt{s} = 0.5$  TeV and  $L = 10^{34} - 10^{35} \text{ cm}^{-2} \text{ s}^{-1}$ , and Linac-Ring type  $ep$  collider (NLC  $\times$  LHC) with  $\sqrt{s} = 3.7$  TeV and  $L = 10^{31} - 10^{32} \text{ cm}^{-2} \text{ s}^{-1}$  (see [1] and references therein). Even though the last one has a lower luminosity it can provide better conditions for investigations of a lot of phenomena comparing to NLC due to the essentially higher center of mass energy and LHC due to more clear environment. For this reason, different phenomena (compositeness, SUSY, etc.) should be analyzed taking into account all three type of colliders.

The fundamental questions left open by the Standard Model (SM), such as the number of fermion families, the fermion masses and the mixings, are addressed by the composite models [2]. In the framework of composite models of quarks and leptons, constituents of known fermions interact by means of new interactions. A non-trivial substructure of known fermions leads to a rich spectrum of excited states [3, 4]. Phenomenologically, an excited lepton is defined to be a heavy lepton which shares leptonic quantum numbers with one of the existing leptons. Charged ( $e^*$ ,  $\mu^*$  and  $\tau^*$ ) and neutral ( $\nu_e^*$ ,  $\nu_\mu^*$  and  $\nu_\tau^*$ ) excited leptons are predicted by composite models where leptons and quarks have substructure.

In this paper, we compare the potential of the machines mentioned above to search for the single production of excited electrons. Current limits on the mass of the excited electron are [5]:  $m_* > 100 \text{ GeV}$  from LEP (pair production),  $m_* > 223 \text{ GeV}$  from HERA and  $m_* > 300 \text{ GeV}$  from LEP (indirect). Single production mechanism extends the search potential up to masses close to the subprocess center of mass energies  $\sqrt{s}$  of the colliders.

The interaction between an excited electron, gauge bosons and the first SM family leptons is described by  $SU(2) \times U(1)$  invariant lagrangian [4]

$$L = \frac{1}{2\Lambda} \bar{l}_R^* \sigma^{\mu\nu} \left[ fg \frac{\vec{\tau}}{2} \cdot \vec{W}_{\mu\nu} + f' g' \frac{Y}{2} B_{\mu\nu} \right] l_L + h.c.$$

where  $\Lambda$  is the scale of the new physics responsible for the existence of excited leptons;  $W_{\mu\nu}$  and  $B_{\mu\nu}$  are the field strength tensors;  $\vec{\tau}$  denotes the Pauli matrices,  $Y = -1/2$  is the hypercharge;  $g$  and  $g'$  are the SM gauge couplings of  $SU(2)$  and  $U(1)$ , respectively; the constants  $f$  and  $f'$  are the scaling factors for the corresponding gauge couplings. In these expressions,  $\sigma^{\mu\nu} = i(\gamma^\mu \gamma^\nu - \gamma^\nu \gamma^\mu)/2$  where  $\gamma^\mu$  are the Dirac matrices.

For an excited electron, three decay modes are possible: radiative decays  $e^* \rightarrow e\gamma$ , charged current decays  $e^* \rightarrow \nu W$ , neutral currents decays  $e^* \rightarrow eZ$ . Neglecting ordinary lepton masses the decay widths are obtained as

$$\Gamma(e^* \rightarrow lV) = \frac{\alpha m_*^3}{4\Lambda^2} f_V^2 \left( 1 - \frac{m_V^2}{m_*^2} \right)^2 \left( 1 + \frac{m_V^2}{2m_*^2} \right)$$

where  $f_\gamma = -(f + f')/2$ ,  $f_W = f/(\sqrt{2} \sin \theta_W)$  and  $f_Z = (-f \cos^2 \theta_W + f' \sin^2 \theta_W)/2$ . The total decay width  $\Gamma$  of the excited electron and the relative branching ratios (BR) into ordinary lepton and gauge bosons  $\gamma, Z, W$  are given in

\*Electronic address: [ocakir@science.ankara.edu.tr](mailto:ocakir@science.ankara.edu.tr)

†Electronic address: [saleh@gazi.edu.tr](mailto:saleh@gazi.edu.tr)

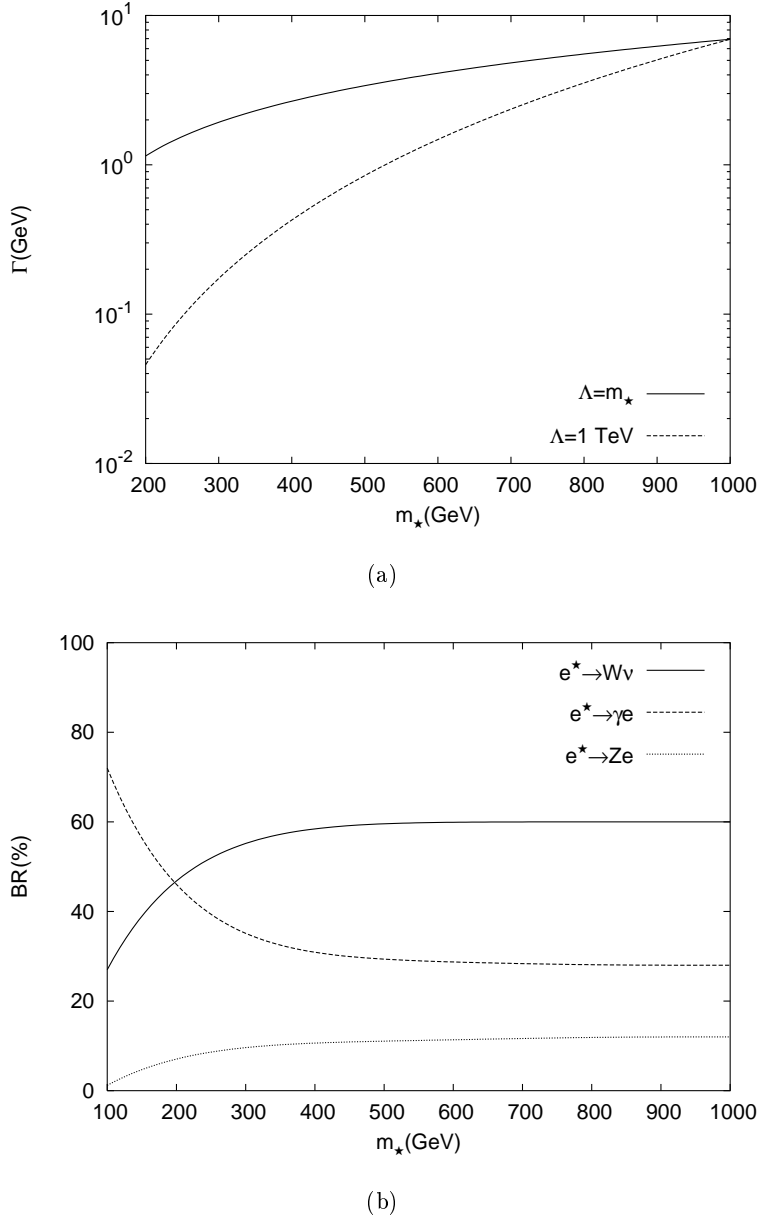


Figure 1: (a) The decay width  $\Gamma$  in GeV of excited electron for the scale  $\Lambda = 1 \text{ TeV}$  and  $\Lambda = m_*$  with the couplings  $f = f' = 1$ , and (b) the branching ratios BR (%) depending on the mass of excited electron for  $f = f' = 1$ .

Fig. 1. For a comparison, in Fig. 1(a) we show the total decay widths of excited electron for  $\Lambda = m^*$  and  $\Lambda = 1 \text{ TeV}$ , which are commonly used for the new physics scale. For large values of the excited electron mass, the branching ratio for the individual decay channels reaches to the constant values 60% for the  $W$ -channel, 12% for the  $Z$ -channel and 28% for the photon channel. The branching ratios in these different modes depend on the relative values of  $f$  and  $f'$ . For  $f = f'$ , the radiative decay is allowed for excited electron whereas it is forbidden for excited neutrino.

## II. SINGLE PRODUCTION OF EXCITED ELECTRONS

We analyze the potentials of the NLC, NLC $\otimes$ LHC and LHC machines to search for excited electrons via the single production reactions

$$e^+ e^- \rightarrow e^{\pm*} e^\mp$$

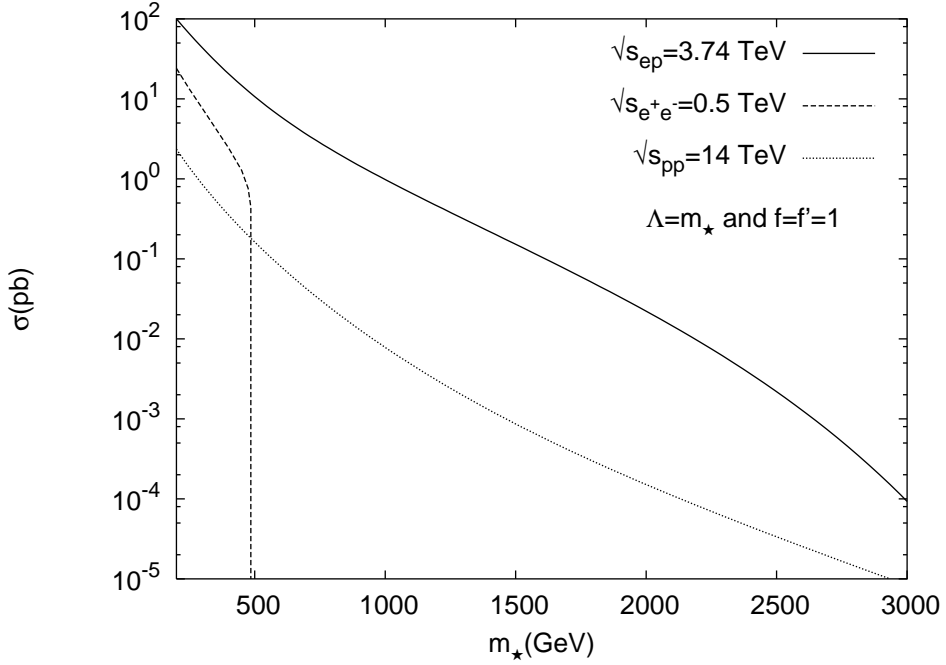


Figure 2: The total cross sections for the single production of excited electron at  $e^-e^+$  collider with  $\sqrt{s} = 0.5$  TeV,  $ep$  collider with  $\sqrt{s} = 3.74$  TeV and  $pp$  collider with  $\sqrt{s} = 14$  TeV.

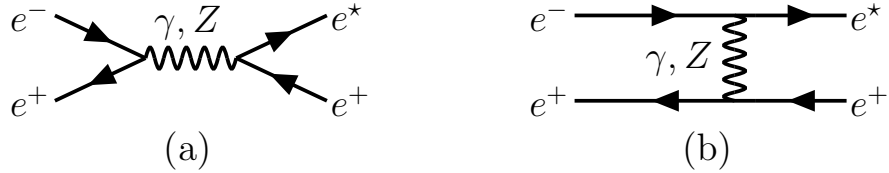


Figure 3: Excited electron production at  $e^-e^+$  colliders through the (a)  $s$ -channel and (b)  $t$ -channel exchange diagrams.

$$e^- p \rightarrow e^{-\star} q(\bar{q}) X$$

$$pp \rightarrow e^{\pm\star} e^\mp X \quad \text{and} \quad pp \rightarrow e^{+(-)\star} \nu(\bar{\nu}) X$$

with subsequent decay of excited electron into photon and an electron. Therefore, we deal with the process  $e^+e^- \rightarrow \gamma e^\pm e^\mp$ , and subprocesses  $e^-q(\bar{q}) \rightarrow \gamma e^-q(\bar{q})$ ,  $q\bar{q} \rightarrow \gamma e^\pm e^\mp$  and  $q\bar{q}' \rightarrow \gamma e^{+(-)}\nu(\bar{\nu})$ . The signal and background were simulated at the parton level by using the program CompHEP 4.2 [5]. In our calculations we used the parton distribution functions library CTEQ6L [6] with the factorization scale  $Q^2 = \hat{s}$ .

For a comparison of different colliders, the signal cross sections for the processes given above are presented in Fig. 2 assuming the scale  $\Lambda = m_*$  and the coupling parameters  $f = f' = 1$ .

#### A. $e^-e^+$ Collider

High energy electron-positron collisions constitute an excellent environment for the search for excited leptons. We examine the single production of excited electrons ( $e^*$ ) at  $e^-e^+$  with  $\sqrt{s} = 500$  GeV, through the process  $e^-e^+ \rightarrow e^{\pm\star} e^\mp \rightarrow e^{\pm} e^\mp \gamma$ . The Feynman diagram for the process  $e^-e^+ \rightarrow e^{-\star} e^+$  is shown in Fig. 3.

We applied to this process the following acceptance cuts

$$p_T^{e,\gamma} > 20 \text{ GeV}$$

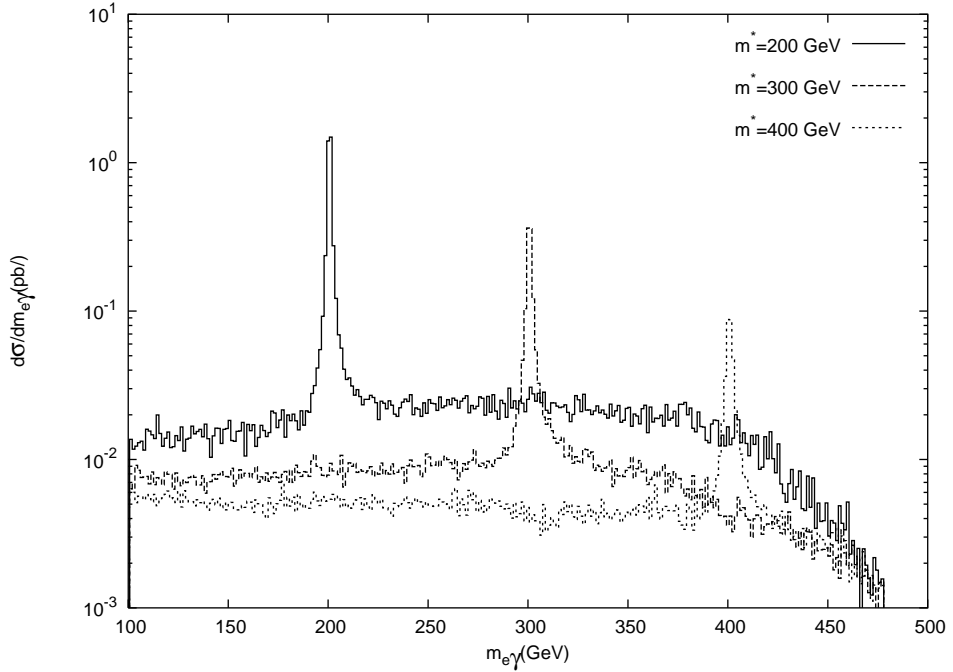


Figure 4: Invariant mass  $m_{e\gamma}$  distribution of signal (the scale  $\Lambda = m_*$  and the coupling parameters  $f = f' = 1$ ) and background at  $e^+e^-$  colliders.

$$|\eta_{e^\pm, \gamma}| < 2.5$$

$$\Delta R_{(e^+e^-), (e^\pm\gamma)} > 0.4$$

where  $p_T$  is the transverse momentum of the visible particle.  $\eta$  stands for the pseudo-rapidity of the visible particles and  $\Delta R = \sqrt{\Delta\eta^2 + \Delta\phi^2}$  is the separation between two of them. After applying these cuts, the SM background cross section is found to be  $\sigma = 1.93$  pb. Fig. 4 shows the invariant mass  $m_{e\gamma}$  distribution in the reaction  $e^+e^- \rightarrow e^+e^-\gamma$  for the SM and with the inclusion of an excited electron with masses  $m_* = 200$  GeV,  $m_* = 300$  GeV,  $m_* = 400$  GeV and  $f = f' = 1$ .

A natural way to extract the excited electron signal, and at the same time suppress the SM backgrounds, is to impose a cut on the  $e\gamma$  invariant mass. Therefore, we introduced the cut

$$|m_{e^\pm\gamma} - m_*| < 25 \text{ GeV}$$

for considered excited electron mass range. In Table I, we have presented the signal (for  $f = f' = 1$ ) and background cross sections in  $e\gamma$  invariant mass bins since the signal is concentrated in a small region proportional to the invariant mass resolution. In order to examine the potential of the collider to search for the excited electron, we defined the statistical significance  $SS$  of the signal

$$SS = \frac{|\sigma_{S+B} - \sigma_B|}{\sqrt{\sigma_B}} \sqrt{L_{int}}$$

where  $L_{int}$  is the integrated luminosity of the collider. The values of  $SS$  evaluated at each excited electron mass points are shown in the last column of Table I. As seen from the Table I the calculated  $SS$  values are higher than 5 up to the center of mass energy of the NLC. For various coupling parameters  $f (= f')$ , we give the  $SS$  values in Fig. 5.

## B. $ep$ Collider

The Feynman diagrams for the subprocess  $eq \rightarrow e^*q$  and  $e\bar{q} \rightarrow e^*\bar{q}$  are shown in Fig. 6. After the acceptance cuts

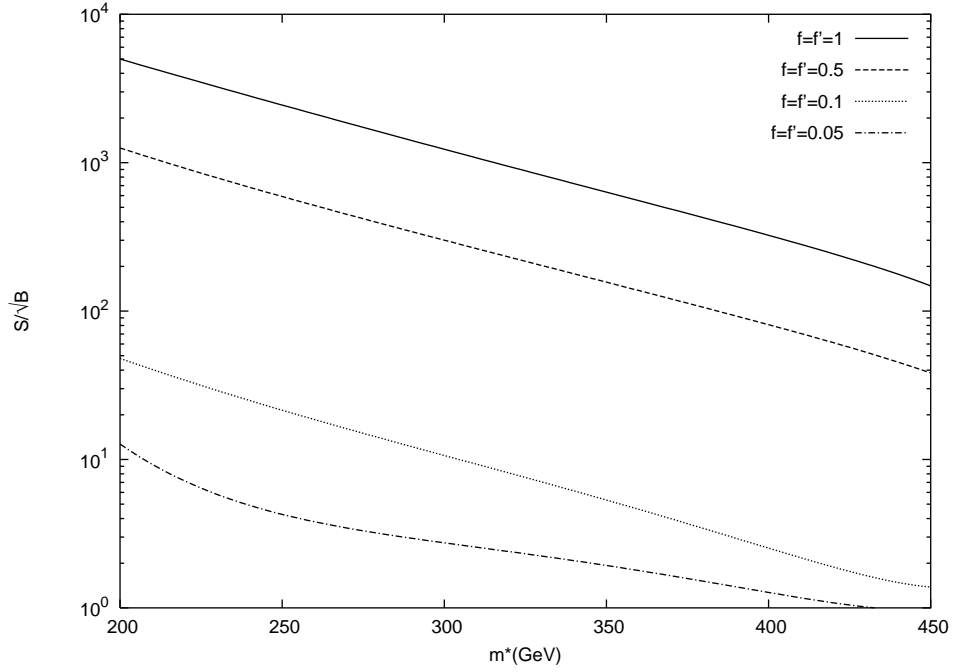


Figure 5: Statistical significance depending on the excited electron mass for  $\Lambda = m_*$  and different coupling parameters at the NLC.

Table I: The cross sections of the excited electron signal and relevant backgrounds after the initial cuts and the cuts  $|m_{e\gamma} - m^*| < 25$  GeV at  $e^-e^+$  collider with  $\sqrt{s} = 0.5$  TeV and  $L_{int} = 10^5 \text{ fb}^{-1}$ .

$m^*(\text{GeV})$	$\sigma_{S+B}(\text{pb})$	$\sigma_B(\text{pb})$	$SS$
200	$5.93 \times 10^0$	$1.35 \times 10^{-1}$	4992.0
250	$3.27 \times 10^0$	$1.68 \times 10^{-1}$	2395.8
300	$1.95 \times 10^0$	$2.02 \times 10^{-1}$	1226.9
350	$1.14 \times 10^0$	$2.26 \times 10^{-1}$	606.9
400	$6.49 \times 10^{-1}$	$1.86 \times 10^{-1}$	185.4
450	$3.17 \times 10^{-1}$	$1.16 \times 10^{-1}$	81.3

the total SM background cross section is obtained as  $\sigma_B = 4.29$  pb. Fig. 7 shows the invariant mass  $m_{e\gamma}$  distribution in the reaction  $e^-q \rightarrow e^-\gamma q$  for the SM background and the signal (for  $f = f' = 1$ ) with the inclusion of an excited electron with masses  $m_* = 200$  GeV,  $m_* = 400$  GeV,  $m_* = 800$  GeV and  $m_* = 1200$  GeV.

In Table II, we present the signal and background cross sections in  $e\gamma$  invariant mass bins satisfying the condition  $|m_{e-\gamma} - m_*| < 25$  GeV for  $m_* = 200 - 1200$  GeV and  $|m_{e-\gamma} - m_*| < 50$  GeV for  $m_* = 1200 - 2500$  GeV. For various coupling parameters  $f (= f')$ , we show the mass dependence of the  $SS$  in Fig. 8.



Figure 6: Single production of excited electrons at  $ep$  colliders through the subprocesses (a)  $eq \rightarrow e^*q$  and (b)  $e\bar{q} \rightarrow e^*\bar{q}$ .

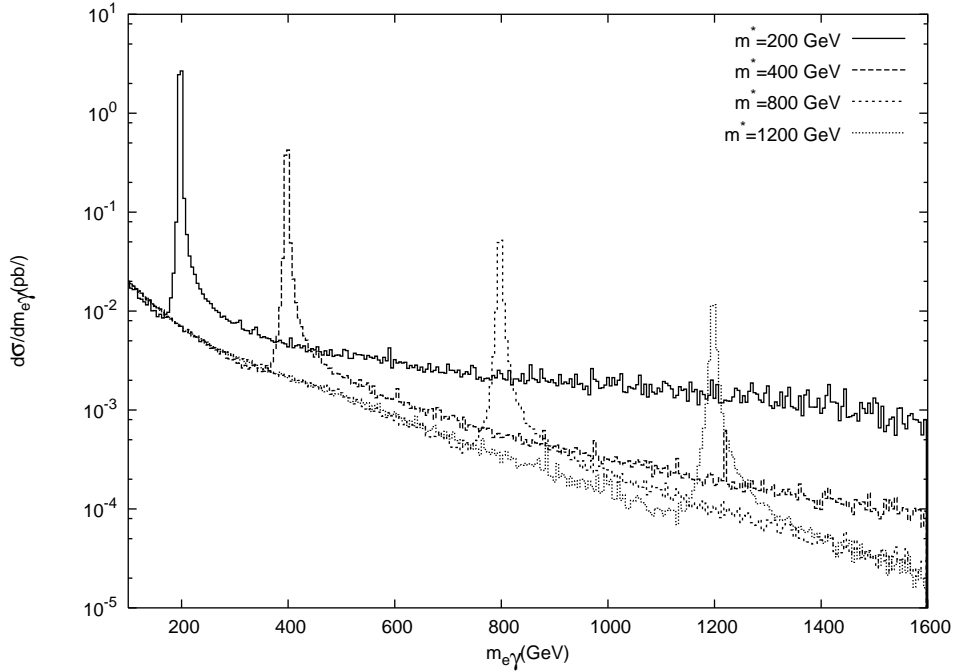


Figure 7: Invariant mass  $m_{e\gamma}$  distribution of signal and background at  $e^-p$  colliders.

Table II: The cross sections of the signal and relevant backgrounds at  $e^-p$  collider with  $\sqrt{s} = 3.74$  TeV and  $L_{int} = 100 \text{ pb}^{-1}$ .

Mass, GeV	$\Delta\sigma_{S+B}(\text{pb})$	$\Delta\sigma_B(\text{pb})$	SS
200	$1.55 \times 10^1$	$5.03 \times 10^{-1}$	2117.5
400	$1.32 \times 10^0$	$1.02 \times 10^{-1}$	696.5
600	$6.68 \times 10^{-1}$	$3.37 \times 10^{-2}$	345.4
800	$2.78 \times 10^{-1}$	$1.25 \times 10^{-2}$	237.1
1000	$1.25 \times 10^{-1}$	$4.44 \times 10^{-3}$	181.6
1200	$6.23 \times 10^{-2}$	$1.83 \times 10^{-3}$	141.3
1500	$1.82 \times 10^{-2}$	$1.17 \times 10^{-3}$	50.2
2000	$5.63 \times 10^{-3}$	$1.16 \times 10^{-3}$	13.1
2500	$2.01 \times 10^{-3}$	$1.16 \times 10^{-3}$	2.5

### C. $pp$ Collider

At the LHC, the single production of excited electrons takes place through the subprocesses  $q\bar{q} \rightarrow Z/\gamma \rightarrow e^\pm e^{\mp*} \rightarrow e^\pm e^\mp \gamma$  and  $q\bar{q}' \rightarrow W^\mp \rightarrow \nu e^{\mp*} \rightarrow \nu e^\mp \gamma$  via the Drell-Yan mechanism. The diagrams related to these subprocesses are shown in Fig. 9. After the acceptance cuts the total SM background cross sections are obtained as  $\sigma_B = 1.16 \text{ pb}$  for the process  $pp \rightarrow e^+e^-\gamma X$  and  $\sigma_B = 1.35 \text{ pb}$  for  $pp \rightarrow \nu e^-\gamma X$ .

Fig. 10 shows the invariant mass  $m_{e\gamma}$  distributions in the reactions  $pp \rightarrow e^+e^-\gamma X$  and  $pp \rightarrow \nu e^-\gamma X$  for the SM background and the signal (for  $f = f' = 1$ ) with the inclusion of an excited electron with masses  $m_* = 200 \text{ GeV}$ ,  $m_* = 400 \text{ GeV}$ ,  $m_* = 800 \text{ GeV}$  and  $m_* = 1200 \text{ GeV}$ . In Table III, we present the signal and background cross sections in  $e\gamma$  invariant mass bins satisfying the condition  $|m_{e-\gamma} - m_*| < 25 \text{ GeV}$  for  $m_* = 200 - 1200 \text{ GeV}$  and  $|m_{e-\gamma} - m_*| < 50 \text{ GeV}$  for  $m_* = 1200 - 2500 \text{ GeV}$ . Statistical significance SS are shown in Fig. 11 for (a)  $pp \rightarrow e^+e^-\gamma X$  and (b)  $pp \rightarrow \nu e^-\gamma X$  processes with different couplings  $f (= f')$ .

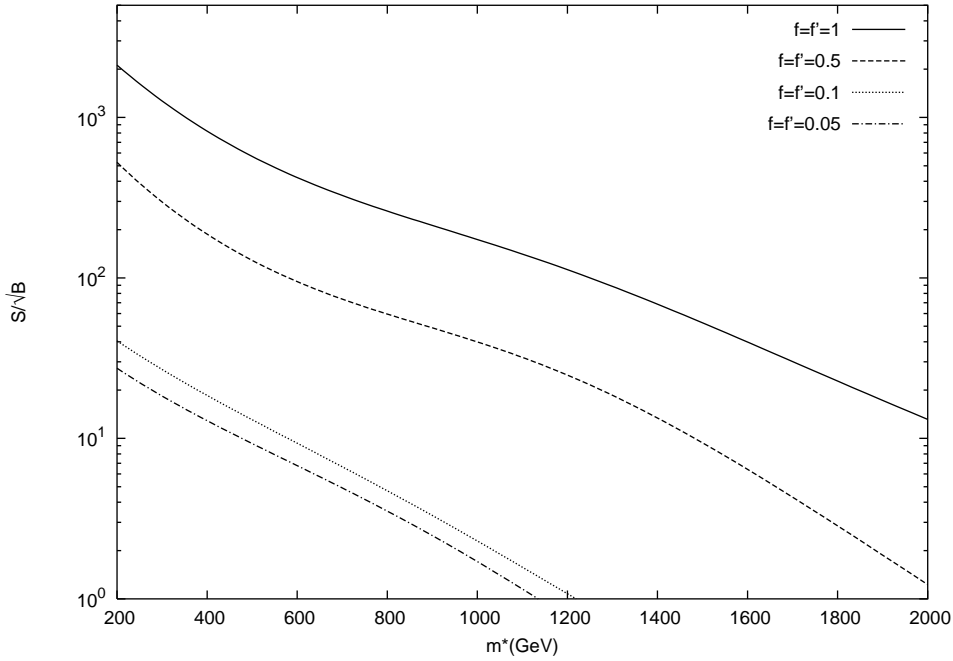


Figure 8: Statistical significance depending on the excited electron mass for different coupling parameters for the process  $e^- p \rightarrow e^{-*} q(\bar{q}) X$  at the NLC  $\otimes$  LHC.

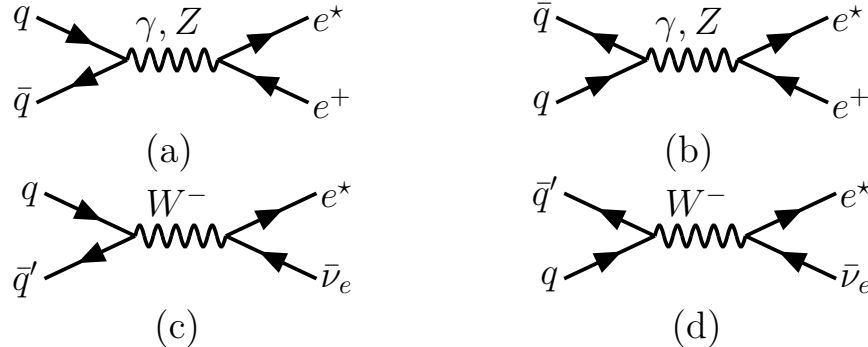


Figure 9: Excited electron production via the (a,b) photon and  $Z$ -boson exchange, and (c,d)  $W^-$ -boson in the  $s$ -channel diagrams at hadron colliders.

Table III: The cross sections of the signal and relevant backgrounds at  $pp$  collider with  $\sqrt{s} = 14$  TeV and  $L_{int} = 10^5 \text{ pb}^{-1}$ . The statistical significance  $SS$  are given for the coupling  $f = f' = 1$  and the scale  $\Lambda = m^*$ .

Final states $\rightarrow$	$e^- e^+ \gamma$			$e^- \bar{\nu} \gamma$		
	Mass, GeV	$\sigma_{S+B}(\text{pb})$	$\sigma_B(\text{pb})$	SS	$\sigma_{S+B}(\text{pb})$	$\sigma_B(\text{pb})$
200	$2.33 \times 10^{-1}$	$1.29 \times 10^{-2}$	613.6	$2.98 \times 10^{-1}$	$9.79 \times 10^{-4}$	3003.8
400	$2.24 \times 10^{-2}$	$1.79 \times 10^{-4}$	524.4	$2.52 \times 10^{-2}$	$5.98 \times 10^{-5}$	1027.5
800	$1.67 \times 10^{-3}$	$8.01 \times 10^{-5}$	56.1	$1.65 \times 10^{-3}$	$2.28 \times 10^{-5}$	107.7
1200	$3.13 \times 10^{-4}$	$1.56 \times 10^{-5}$	23.8	$2.91 \times 10^{-4}$	$1.29 \times 10^{-5}$	24.4
1600	$7.63 \times 10^{-5}$	$5.75 \times 10^{-6}$	9.3	$7.00 \times 10^{-5}$	$5.81 \times 10^{-6}$	8.4
2000	$2.26 \times 10^{-5}$	$1.24 \times 10^{-6}$	6.1	$1.97 \times 10^{-5}$	$1.46 \times 10^{-6}$	4.8
2500	$6.27 \times 10^{-6}$	$7.35 \times 10^{-7}$	2.0	$4.97 \times 10^{-6}$	$6.14 \times 10^{-7}$	1.7

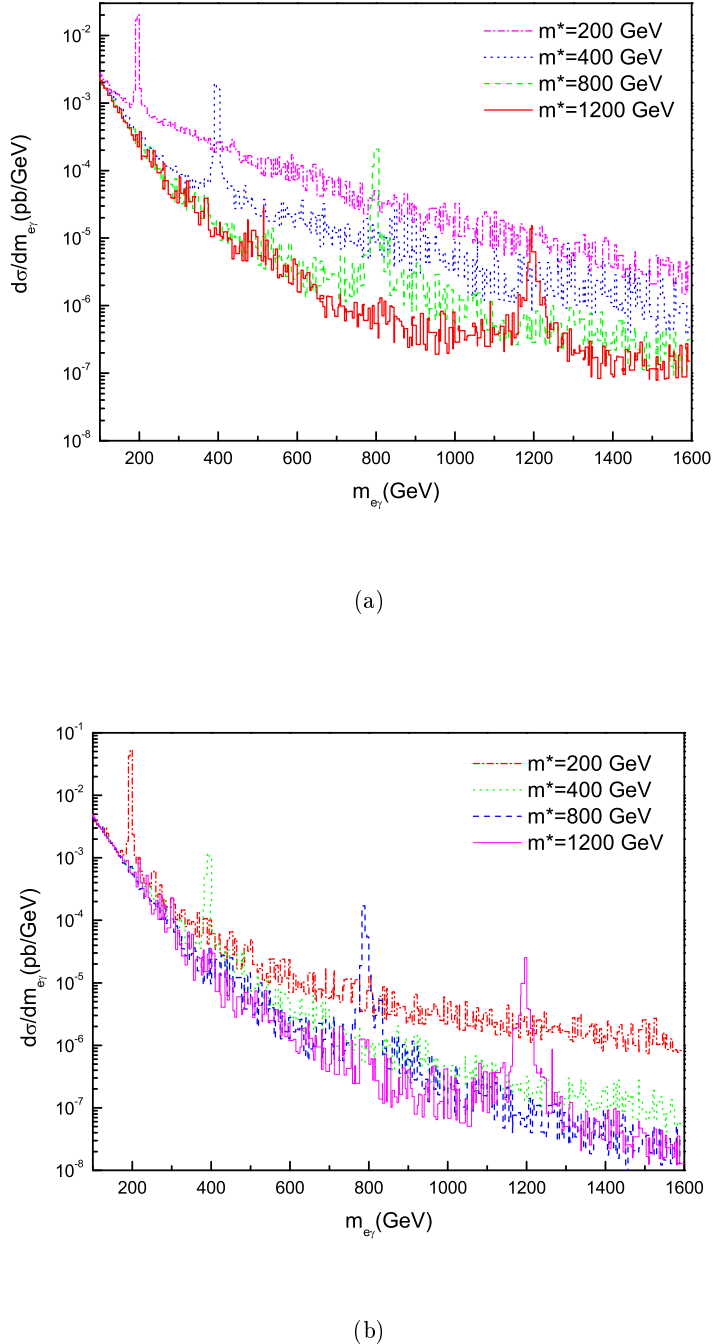


Figure 10: Invariant mass  $m_{e\gamma}$  distribution of signal and background for the processes (a)  $pp \rightarrow e^+e^-\gamma X$  and (b)  $pp \rightarrow \nu e^-\gamma X$  at  $pp$  colliders.

### III. CONCLUSION

Since the cross section for the signal is proportional to  $1/\Lambda^2$ , various choices of the  $\Lambda$ , i.e. in this study we have chosen  $\Lambda = m_*$ , will lead to the changes in the cross sections as  $(m_*/\Lambda)^2$ . For  $\Lambda = 1$  TeV, we need to multiply the cross sections by a factor  $[m_*(\text{TeV})]^2$  at every mass values of excited electrons. This factor also extends the attainable

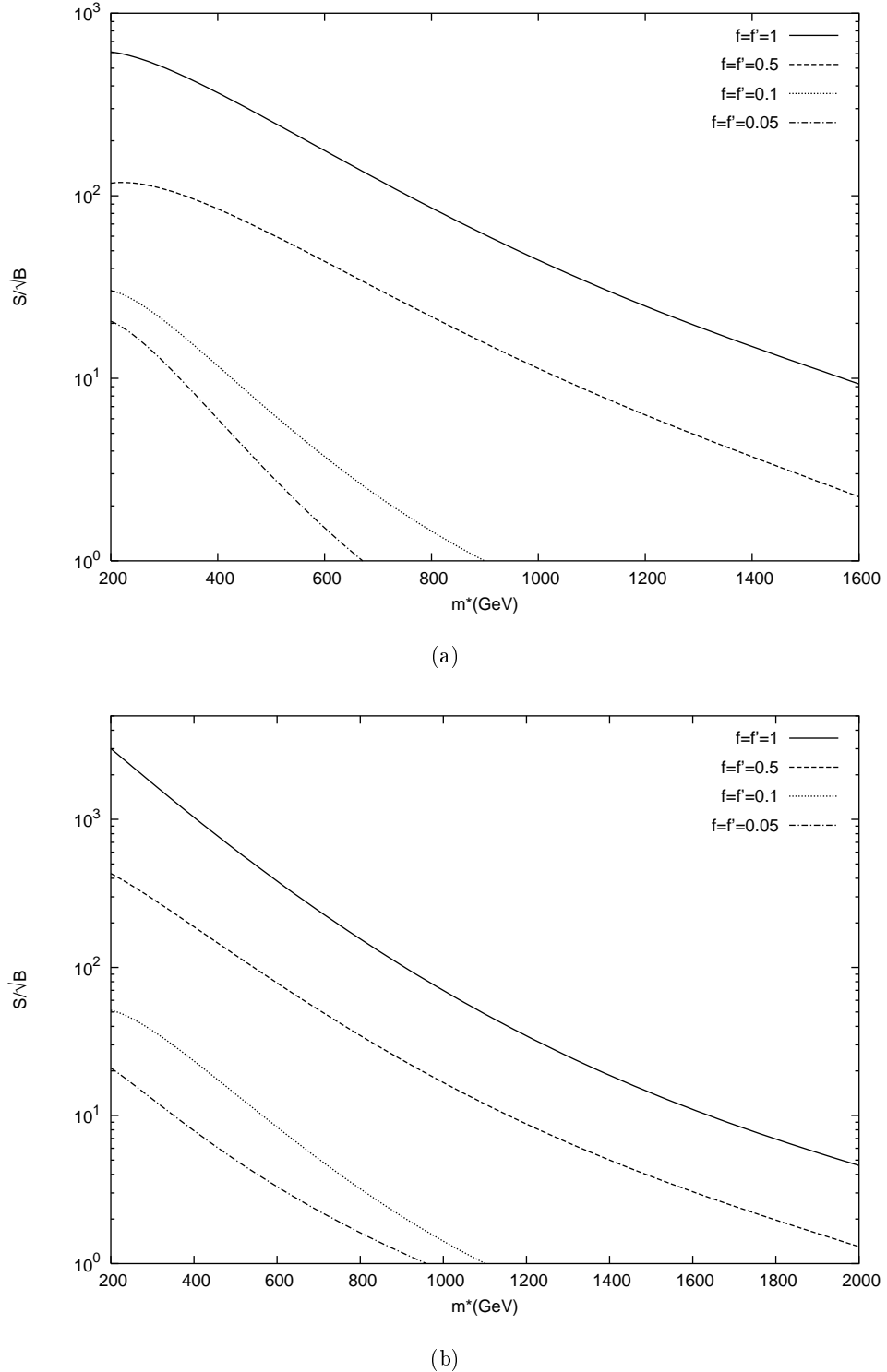


Figure 11: Statistical significance depending on the excited electron mass for process (a)  $pp \rightarrow e^+ e^- \gamma X$  and (b)  $pp \rightarrow \nu e^- \gamma X$  with different couplings  $f (= f')$  at the LHC.

mass limits for  $m_\star > 1\text{TeV}$ . Our analysis show that for  $f = f' = 1$  NLC can discover excited electron in  $e^* \rightarrow e\gamma$  decay mode up to the kinematical limit, while NLC  $\otimes$  LHC and LHC can reach much higher mass values, namely 2300 GeV and 1900 GeV, respectively. For  $f = f' = 0.05$  discover limits are: 240 GeV at NLC, 650 GeV at NLC  $\otimes$  LHC and 450 GeV at LHC.

### Acknowledgments

This work is partially supported by Turkish State Planning Committee under the Grants No 2002K120250 and 2003K120190.

---

- [1] S. Sultansoy, Eur. Phys. J. C (2004) DOI 10.1140/epjcd/s2004-03-1716-2; <http://eps2003.physik.rwth-aachen.de/data/talks/parallel/15Accelerator/15Sultansoy.ppt>
- [2] H. Terazawa, Y. Chikashige and K. Akama, Phys. Rev. D **15**, 480 (1977); Y. Ne'eman, Phys. lett. B **82**, 69 (1979); H. Terazawa, M. Yasue, K. Akama and M. Hayashi, Phys. Lett. B **112**, 387 (1982).
- [3] F. M. Renard, Il Nuovo Cimento A **77**, 1 (1983); A. De Rujula, L. Maiani and R. Petronzio, Phys. Lett. B **140**, 253 (1984); E.J. Eichten, K.D. Lane and M.E. Peskin, Phys. Rev. D **50**, 811 (1983).
- [4] U. Baur, M. Spira and P.M. Zerwas, Phys. Rev. D **42**, 815 (1990).
- [5] K. Hagiwara et al., Particle Data Group, Phys. Rev. D **66**, 010001 (2002).
- [6] A. Pukhov *et al.*, hep-ph/9908288 (1999).
- [7] H.L. Lai et al., CTEQ Collab., Phys. Rev. D **51**, 4763 (2000).